



Article

In-Field Route Planning Optimisation and Performance Indicators of Grain Harvest Operations

Michael Nørremark, René Søndergaard Nilsson and Claus Aage Grøn Sørensen

Special Issue

The Future of Agriculture: Towards Automation

Edited by
Prof. Dr. Claus Grøn Sørensen



<https://doi.org/10.3390/agronomy12051151>

Article

In-Field Route Planning Optimisation and Performance Indicators of Grain Harvest Operations

Michael Nørremark ^{1,*}, René Søndergaard Nilsson ²  and Claus Aage Grøn Sørensen ¹

¹ Department of Electrical and Computer Engineering, Aarhus University, DK-8200 Aarhus, Denmark; claus.soerensen@ece.au.dk

² Research & Advanced Engineering, AGCO A/S, DK-8930 Randers, Denmark; rene.nilsson@agcocorp.com

* Correspondence: michael.norremark@ece.au.dk

Abstract: Operational planning, automation, and optimisation of field operations are ways to sustain the production of food and feed. A coverage path planning method mitigating the optimisation and automation of harvest operations, characterised by capacity limitations and features derived from real world scenarios, is presented. Although prior research has developed similar methods, no such methodologies have been developed for (i) multiple field entrances as line segments, (ii) the feasibility of stationary and on-the-go unloading in the headland and main field, (iii) unloading timing independent of the full bin level of the harvester, and (iv) the transport unit operational time outside the field. To find the permutation that best minimises the costs in time and distance, an artificial bee colony (ABC) algorithm was used as a meta-heuristic optimisation method. The effectiveness of the method was analysed by generating simulated operational data and by comparing it to recorded data from seven fields ranging in size (5–26 ha) and shape. The implementation of controlled traffic farming (CTF) in the coverage path planning method, but not with the recorded data, resulted in a reduced risk of soil compaction of up to 25%, and a reduction in the in-field total travel distance of up to 15% when logistics was optimised simultaneously for two transport units. A 68% increase in the full load frequency of transporting vehicles and a 14% reduction in the total number of field to storage transports was observed. For fields located at outermost edges of the storage facility (>5 km), the increase in full load frequency, average load level, and decrease in in-field travel distance resulted in a reduction in fuel consumption by 7%. Embedding the developed coverage path planning software as a service will improve the sustainability of harvest operations including a fleet of one to many harvesting and transporting units, as the system in front of the vehicle operator calculates and displays all required actions from the operator.

Keywords: agricultural field operations optimisation; coverage path planning; fleet management; artificial bee colony; capacitated arc routing problem



Citation: Nørremark, M.; Nilsson, R.S.; Sørensen, C.A.G. In-Field Route Planning Optimisation and Performance Indicators of Grain Harvest Operations. *Agronomy* **2022**, *12*, 1151. <https://doi.org/10.3390/agronomy12051151>

Academic Editor: Mario Cunha

Received: 16 March 2022

Accepted: 28 April 2022

Published: 10 May 2022

Publisher's Note: MDPI stays neutral with regard to jurisdictional claims in published maps and institutional affiliations.



Copyright: © 2022 by the authors. Licensee MDPI, Basel, Switzerland. This article is an open access article distributed under the terms and conditions of the Creative Commons Attribution (CC BY) license (<https://creativecommons.org/licenses/by/4.0/>).

1. Introduction

Mechanical engineering and optimisation has been key to increasing the productivity and efficiency of agricultural machinery for decades. This is related to the savings resulting from the improved mechanical functionality of agricultural machinery. A transformation is currently taking place, as agricultural machinery technology is enabling the deployment of automation. Over the last decade, manufacturers of agricultural machinery have been removing functions from the operator and relegating those to machine controls. This new technological trend has an impact on agricultural machinery and the way it is designed [1]. The next step is not just automation in machine controls, but in technology controlling and executing in-field decisions—In short, smarter machines doing more of the control and operations by themselves [2–5]. In particular, optimised route and path planning is one of the most important requirements voiced by farm managers and machine contractor managers as an integrated part of advanced fleet management systems for agricultural machinery [3]. Non-working traffic not only causes excessive soil compaction due to

the repetition of turning manoeuvres [6,7], but also increases fuel consumption, labour demands, and operators' workload. Therefore, the selection of an optimised fieldwork pattern and machine configurations for a particular operation plays an important role in the reduction of the non-working distance and time. A preliminary step in this direction of achieving increasing operational efficiency is a renewed focus on the usage of advanced systems both in terms of technology and management measures, for instance, vehicle routing optimisation. Optimal route planning of agricultural machinery on fields can improve field operations when applying liquid fertilizer [8,9], for non-capacitated vehicle route optimisation [10–12] and for the fleet management of multiple vehicles [13–15]. Vehicle routing optimisation are working for fields of different shapes [16,17] and with obstacles [18], and when working in complex-geometry fields that impose restrictions on certain travel paths [19–21]. Apart from improving route efficiency, field coverage planning has also been deployed to reduce soil compaction [22,23] and machine servicing time [24].

Path planning of all vehicles featuring harvest operations is a complex operation that currently relies solely on the operator experience of harvesting and transporting equipment. Inefficient combine harvester and transport unit routing negatively impacts profitability in crop production [25,26]. Crop harvesting operations require precise route guidelines for the fleet of vehicles. Due to the transferring of agricultural bulk products in such operations, it is necessary to take into account the capacity of both the harvesting and transporting equipment. An appropriate approach is to make use of the capacitated vehicle routing problem modelling and identification of the activities that contribute to the reduction of the efficiency and the definition of the actions that take place during the operation. The field efficiency is not a constant value for a given operation. Rather, it is affected by the vehicle manoeuvrability, fieldwork pattern, field shape, field size, crop yield (for harvesting), soil conditions, system capabilities (e.g., the bin size of the harvester and transport units), and the driver's experience. Particularly, the fieldwork pattern is an important factor, since it is variable for a particular operation where the field shape, field conditions, machinery, and crop are given. The fieldwork pattern affects the amount of wasted time due to excessive non-working distance and time during the operation. This has been analysed experimentally and proved in actual operations [27–29] as well as proved using simulation models, e.g., [10,30–33].

The focus of this paper is operational planning of grain harvesting operations, where in-field routing is generated prior to and during the actual execution of the harvesting operations. While there has been great progress in the area of agricultural path planning, a coverage path planning method mitigating the optimisation and automation of harvest operations, characterised by capacity limitations and features derived from real world scenarios has yet to be demonstrated.

The first objective of the research presented in this article is to adapt the artificial bee colony (ABC) algorithm to the capacitated vehicle routing problem to obtain a coverage path planning optimisation method developed for (i) multiple field entrances as line segments, (ii) the feasibility of stationary and on-the-go unloading in the headland and main field, (iii) unloading timing independent of the full bin level of the harvester, and (iv) the transport unit operational time outside the field, with the overall aim to minimise the costs in time and distance of all vehicles featuring a harvest operation. The second objective is to analyse the performance of the coverage path planning method with real field conditions to minimise any practical implementation constraints and compare to current practice of harvest fleet logistics.

The remainder the article is organized as follows. Section 2 reviews the previous approaches related to the optimization of harvest fleet logistics. Section 3 describes the adaption of the ABC algorithm to handle the capacitated arc routing problem (CARP), and accordingly, Section 3 introduces data from the reference farm and presents a scalable and modular proof-of-concept algorithm for optimizing the path planning of multiple vehicles. The comparison of reference (real) and optimized (modeled) performance indicators are presented in Section 4. Finally, the conclusions are presented in Section 5.

2. Literature Review of Harvest Fleet Operation Optimisation Methods

Evans et al. [34] determined the minimum non-working distance for a single harvester by modelling the system considering the harvester capacity constraint, accounting for unloading on-the-go and stationary unloading by deploying the travelling salesman problem to find the best order of traversing all the tracks. The system was optimised by a genetic algorithm operator that was able to optimise the harvest route and provide a feasible solution in real field conditions. Simulation results were validated using irregular field shapes and actual yield data collected from a harvester, resulting in a reduced non-working in-field travel distance between 13.8% and 31.5%. The algorithms did not simultaneously optimise the route and filling of transport units and harvesters and did not plan the paths and unloading strategy for the headland area. Ali et al. [35] proposed a combination of the vehicle routing problem (VRP) and minimum cost network flow problems in order to determine the optimal routes for combine harvesters as well as feasible positions for grain transfer between the combine harvesters and transport units. Ali et al. [35] concluded that the capacitated version of metaheuristic operators solving the vehicle routing problem has the highest relevance for harvest-logistics planning. In the capacitated vehicle routing problem (CVRP), each vehicle has a specific capacity, and, once a vehicle reaches its limit, it returns to the depot. The model was able to optimise the harvest route, but many of the assumptions used made it impractical for actual operations. For instance, all of the grain transfer points were at the edge of the field; unloading from the harvester into the transport unit (i.e., on-the-go) was not considered. Harvesting was not modelled as headland operations. Fields were divided into grids, and the harvester was allowed to make turns anywhere in the field. This allowed for the navigation around the in-field obstacles, but was also highly uncommon for the harvesting of crops, because random deviations from tracks or rows consequently require driving on subfield areas with unharvested crops, a practice that generally should be avoided. Bakhtiari et al. [32] applied an approach based on ant colony optimisation for optimal fieldwork coverage plans for harvesting operations using the optimal track sequence principle B-patterns [36]. Specifically, the approach addressed the case where the harvester is unloading to a stationary facility located outside of the field area, or at the field boundary. Results from comparing the optimal plans with conventional plans generated by operators show reductions in the in-field nonworking distance in the range of 19.3–42.1%, while the savings in the total non-working distance were in the range of 18.0–43.8% Bakhtiari et al. [32]. These savings provide a high potential for the implementation of the ant colony optimisation approach for the case of harvesting operations that are not supported by transport equipment for the out-of-the-field removal of the crops. The majority of the technological developments and route planning approaches concern single machines and not multiple-machinery systems. For example, multiple-machinery systems in agricultural field operations include one or more self-propelled or tractor-pulled units and one or more transport units. Using the terminology proposed by Bochtis and Sørensen [37], Bochtis et al. [38], collaborative field operations are executed by one or more primary units (PUs) performing the main work task and one or more service units (SUs) supporting one or more PUs. For example, in a harvesting operation, single or multiple self-propelled harvesters may be supported by transport unit(s) used for the out-of-the-field removal of agricultural bulk products. Bochtis et al. [38], using the abstraction that the PUs are the “customers” in the vehicle routing problem with time windows (VRPTW), showed that operational planning problems related to cooperating PUs and SUs can be cast as instances of the VRPTW and solved by adopting algorithmic approaches developed within this domain. Preliminary results indicate that potential savings include increasing the capacity (ha/h) ranging from 5% to 12%, and reducing non-working distances by up to 50%.

3. Materials and Methods

3.1. Overview

Operational planning for grain harvest operations are particularly challenging because of the high output material flow and handling of the material logistics. Although the presented approach is focused on the case where a path plan is needed to guide a transport unit(s) from its current position to the offloading position next to a combine, a more general terminology will be used, as proposed by Bochtis and Sørensen [37], Bochtis et al. [38]. According to this terminology, cooperative field operations are executed by one or more primary units (PUs) performing the main task and one or more service units (SUs) supporting the PU's. This generalisation also includes the case of input bulk material operations, e.g., seeding and fertilising operations, where a tractor carrying a seeder is supported by transport units carrying the fertilizer and seeds for refilling the application units, as well as the case of output bulk material operations, e.g., harvesting that will be solely pursued in the presented paper. In this paper, the focus is on grain harvest operations with service units and on-the-go unloading between the PUs and SUs, which is a strategy used to achieve the highest possible field efficiency of the PUs. The presented coverage path planning method can generate complete route plans for both PUs and SUs while optimising field efficiency and non-working travel distance. In order to evaluate the potential benefits of the presented coverage path planning method, generated route plans were compared with the recorded data of a single PU and two SUs. Figure 1 shows a flow diagram of the use of recorded data for parametrising the coverage path planning method and for the statistics to determine the effect of optimised route planning for the harvest operation at field level. Initially, recorded data were collected for a set of fields at a test farm. The historical data included a recording of the global position and CAN bus of the PU and a recording of the global position of the tractors pulling the grain transport trailers (SUs). The data were sent wirelessly via a Universal Mobile Telecommunications System (UMTS) network to servers. Recordings of each SU grain load were registered on a weighbridge. Erroneous yield recordings from the PU were removed, and the remaining and valid recordings were calibrated to true grain yield per field. Validated digital yield maps were used as input parameters for the coverage path planning method. Secondly, the collected data were analysed, which generated both input parameters for the coverage path planning method and a data set of quality measures. Next, the coverage path planning method was executed, and a similar data set was generated. The data set from recording and simulation was analysed in the same way, and the generated quality measures could then be compared in a balanced way. The sections below describe the coverage path planning method, data collection, and data analysis in greater detail.

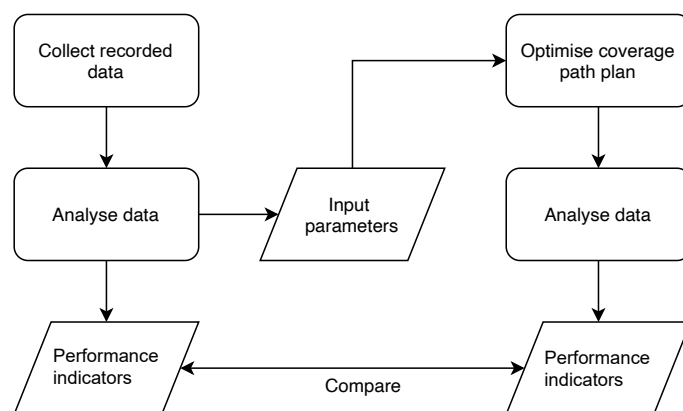


Figure 1. Flow diagram of the data analysis and comparison between the recorded and simulated data derived from the developed coverage path planning method. Input parameters to the coverage path planning method were derived from recorded data and provided the capacity and constraint parameters for the PU and SUs.

3.2. Coverage Path Planning Method

The presented coverage path planning method is generic in the sense that it supports any kind of full-coverage field operation, which has been described in previous work by Nilsson and Zhou [39,40]. The recorded data originate from the grain harvest, so the presented coverage path planning method is applied to grain harvest logistics with the on-the-go unloading and use of SUs, which is an extension of the previous presented method in Nilsson and Zhou [39,40]. Figure 2 shows a high-level flow diagram of the coverage path planning method, including necessary inputs and generated outputs. The method consists of two parts: *field partitioning* and *route generation*.

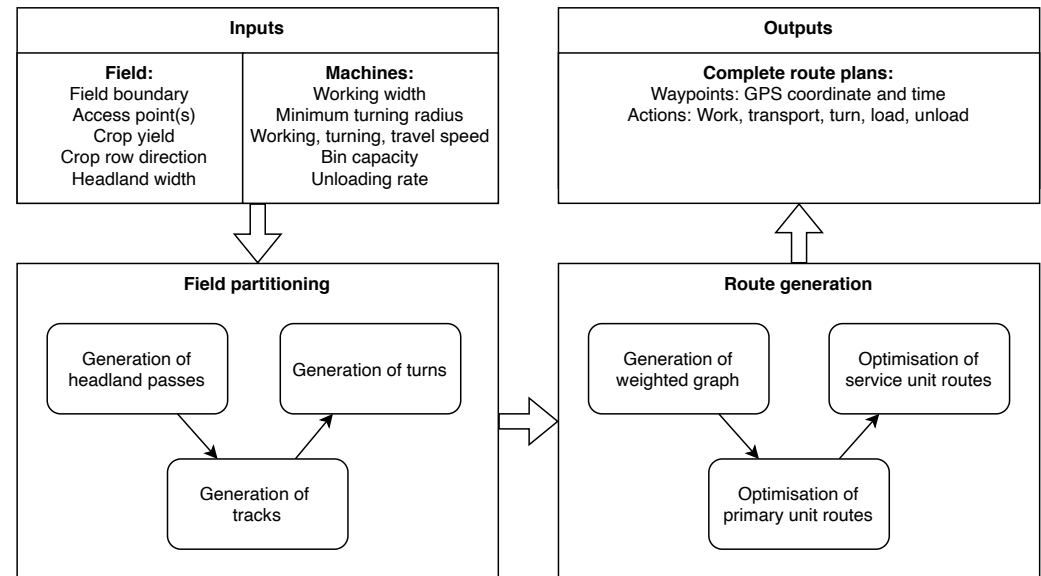


Figure 2. Flow diagram of the coverage path planning method showing the steps from the input of parameters and constraints to arable field partitioning, to a graph representation of the tracks, to a meta-heuristic optimisation, and to the final output as a complete simulation of optimised route plans for the PUs and SUs.

3.2.1. Field Partitioning

Field partitioning was performed according to the geometrical representation method by Zhou et al. [18] and Nilsson and Zhou [40] and refers to a spatial decomposition of the field area into *headland passes* and *tracks* and to the generation of potential turning paths, connecting headland passes, tracks, and field access points. As such, the field partitioning generates the complete road network that all machines are allowed to traverse, while the headland passes and tracks in combination constitute the area that must be harvested. The headland passes are defined as concentric paths, which are generated as inward offsets of the field boundary based on the working width of the PUs and the headland width input, and subsequently smoothed to account for the minimum turning radius (see Figure 3). The tracks are defined as a straight path derived from the crop row direction input, which is propagated across the field in order to generate full coverage of the primary area. The following types of turning manoeuvres are generated based on Dubin turns [41]:

- A2H: Turning manoeuvres from a field access point to a headland pass, allowing machines to enter and exit the field.
- H2H: Turning manoeuvres between two headland passes, near the access points and in field corners.
- T2H: Turning manoeuvres between a track and a headland pass.
- T2T: Turning manoeuvres between two tracks. These are only generated, if there is no direct transition between the two tracks via a headland pass and T2H turns.

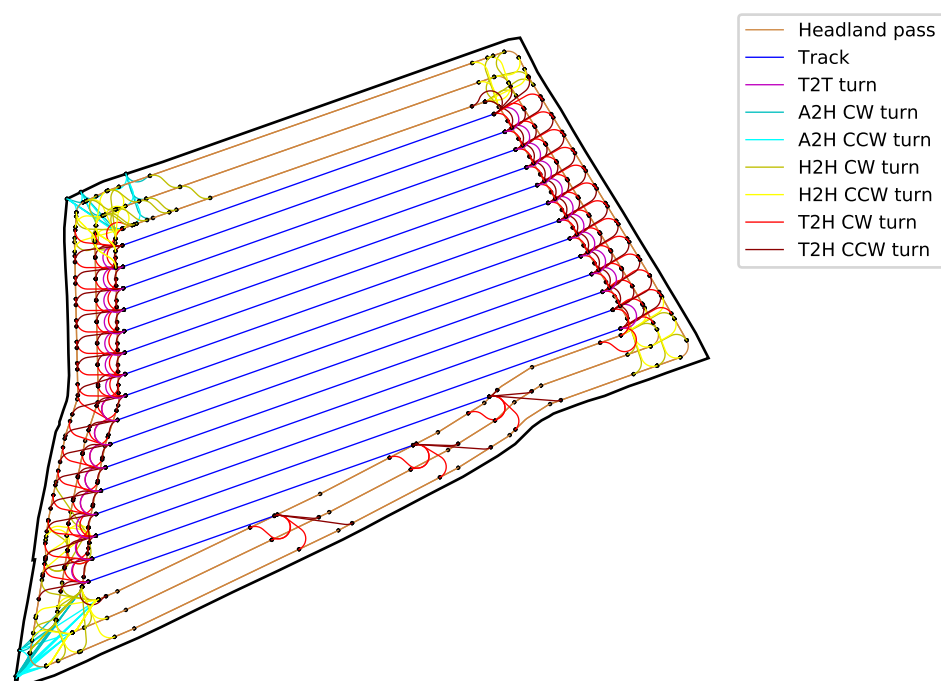


Figure 3. Field partitioning of field No. 4 (Table 1) showing the complete grid of graph vertices (black dots) and arcs, i.e., the path network that all PUs and SUs are allowed to traverse, while the headland passes ('Headland pass') and tracks ('Tracks') which in combination constitutes the area that must be covered by the PU. The following abbreviations in combination explains the illustration of the generated output of all possible turning paths, connecting passes, and field access passes. T: main field track; H: headland; 2: maneuvering between; A: field access; CW: clockwise manoeuvre; CCW: counter clockwise manoeuvre.

All of the turn types are shown in Figure 3, where the turn direction (clockwise (CW)/counterclockwise (CCW)) is also highlighted in order to enhance visualisation and explanation.

Table 1. Geometric data for the seven case study fields including perimeter (m)-to-area (m²) ratio (P/A, m^{−1}) and field area.



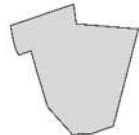


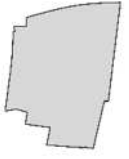

Field No.	Crop	Area [ha]	P/A [m ^{−1}]	Contour
2	Spring barley (<i>Hordeum vulgare</i>)	14.01	0.0132	
4	Spring barley (<i>Hordeum vulgare</i>)	6.43	0.0169	
7	Winter wheat (<i>Triticum aestivum</i>)	21.41	0.0093	
8	Spring barley (<i>Hordeum vulgare</i>)	4.95	0.0221	

Table 1. Cont.

Field No.	Crop	Area [ha]	P/A [m ⁻¹]	Contour
10	Spring barley (<i>Hordeum vulgare</i>)	11.87	0.0154	
12	Winter wheat (<i>Triticum aestivum</i>)	26.47	0.0084	
13	Winter wheat (<i>Triticum aestivum</i>)	16.82	0.0139	

3.2.2. Route Generation

The second part of the method generates routes for both the PUs and SUs. Note that the route generation method for the PUs is described in previous work [40], although the on-the-go unloading and path planning of SUs are not covered by Nilsson and Zhou [40]. As shown in Figure 2, the first step of the route generation method is a graph representation of a field. This step is transforming the field partition to a directed weighted graph $G = (V, A)$, where V is a set of vertices, and A is a set of arcs. Each track, headland pass segment, and turn manoeuvre from the field partition is represented by two arcs (a_{ij}, r_{ij}) with an opposite direction, as illustrated for a simplified field in Figure 4 and for a real field in Figure 3 (field also depicted as satellite image in Figure 5), and associated with a type $t_{ij} \in \{headland, track, turn\}$. This enables that U-turns in the field are not possible and enables Dijkstra's algorithm [42] to calculate the possible and durable paths in the graph. With the graph representation of the field, the coverage path planning problem for the PUs can be described as follows [40]:

$$x^* = \operatorname{argmin}_x f(x, C) \quad (1)$$

such that

$$C_v = \emptyset, \quad (2)$$

$$\forall a_{ij} \in A, t_{ij} \in \{headland, track\} \implies \exists a_{ij} \in x \vee \exists r_{ij} \in x \quad (3)$$

where x^* is the optimal solution, and $f(x, C)$ is the objective function, which evaluates the cost associated with the solution x and the given constraints C . Equation (2) ensures that the set of violated constraints $C_v \subset C$ is empty for the given solution, while Equation (3) guarantees full coverage of all processable tracks in the graph. A solution x comprises a list of arcs and associated timestamped tasks (e.g., transport, turn, actual field work, exit/entry of field, unloading, and loading) for each vehicle.

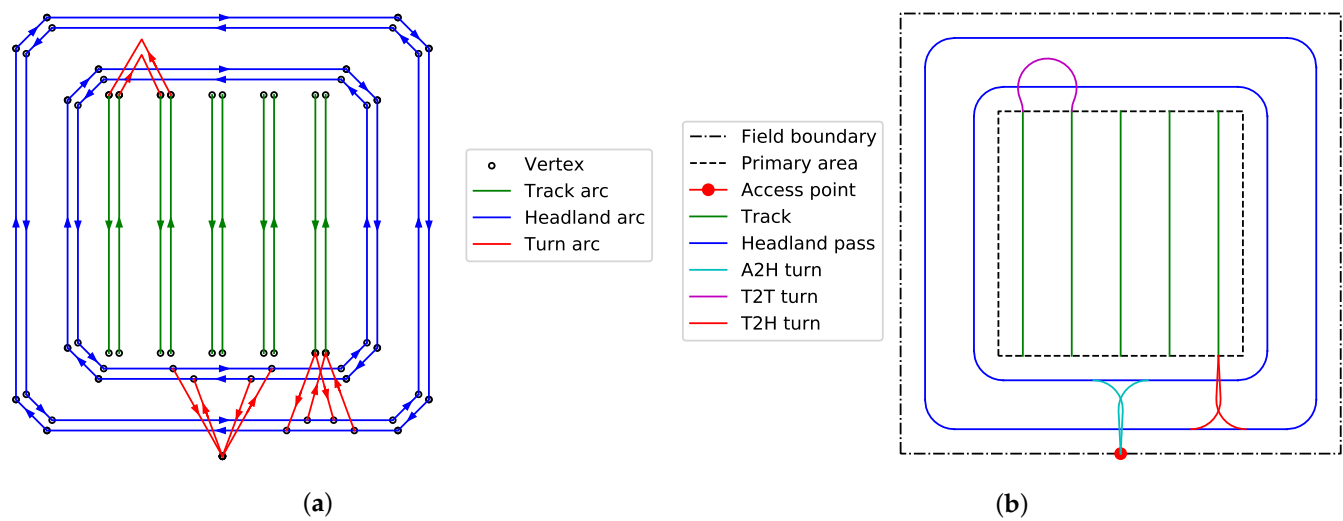


Figure 4. Graph representation (a) and corresponding field partitioning (b) of a simplified field shape showing the outer field boundary and field partitioning into main field and headland area, the complete grid of graph vertices (black dots) and arcs, i.e., all possible path networks, while the headland passes ('Headland arc'/'Headland pass') and tracks ('Track arc'/'Track') which in combination constitutes the area that must be covered by a field operation. The following abbreviations in combination explains the illustration of the generated output of all possible turning paths, connecting passes, and field access passes (b). T: main field track; H: headland; 2: maneuvering between; A: field access; CW: clockwise manoeuvre; CCW: counter clockwise manoeuvre.

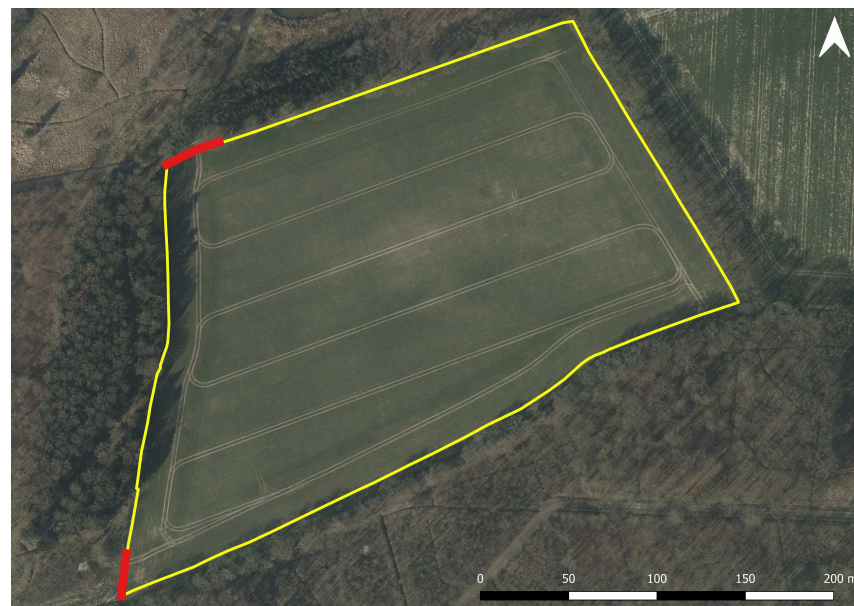


Figure 5. Aerial photograph of the field presented in Figure 3. The field boundary is marked in yellow and field entry/exit segments are marked in red. There are five visible main field traffic lanes and the headland traffic lane is also visible. The field traffic lanes are oriented in the same direction as defined for the field partitioning as illustrated in Figure 3.

For the results presented in this paper, the following constraints are included: field access, distance, tracks only open for traffic after harvest, CTF, headland harvest first, capacities of PUs and SUs, on-the-go unloading, and unloading dimension (the left side of the PU only). The field access constraint determines at which access points each vehicle must start and end the operation, while the distance constraint simply calculates the

total route distance, which is used in the optimisation. The CTF constraint comprises the coercing of the SU(s) to use the field partition of the PU(s). The on-the-go unloading and dimension constraints together require a control of every unloading to enable unload to the left, i.e., that the adjacent track or headland pass to the left of the PU is already harvested.

In addition, it is also the on-the-go unloading constraint, which determines exactly when, where, and how much of the PU bin contents in m^3 is unloaded at each time. In order to address this, (i) the headland width and turning manoeuvres do not always allow turns to the next adjacent track, (ii) any sub-field area is covered to avoid long travelling distances between sub-fields, and (iii), in general, the solution is not always compatible with the constraints defined in the problem formulation. For instance, in non-existing space for an SU for on-the-go unloading, the coverage path planning problem is solved by a constructive algorithm for the headland area and a meta-heuristic algorithm for coverage of the tracks in the primary area. The constructive headland algorithm creates clockwise routes around the headland passes, starting with the outermost headland pass, as illustrated in Figure 6. If it is necessary to unload in the outermost headland, this is performed while it is stationary, since there is no space for an SU on the left side of the PU (outside the field boundary). The rest of the unloading in the inner headland passes are performed while driving, as the already-harvested headlands will allow this.

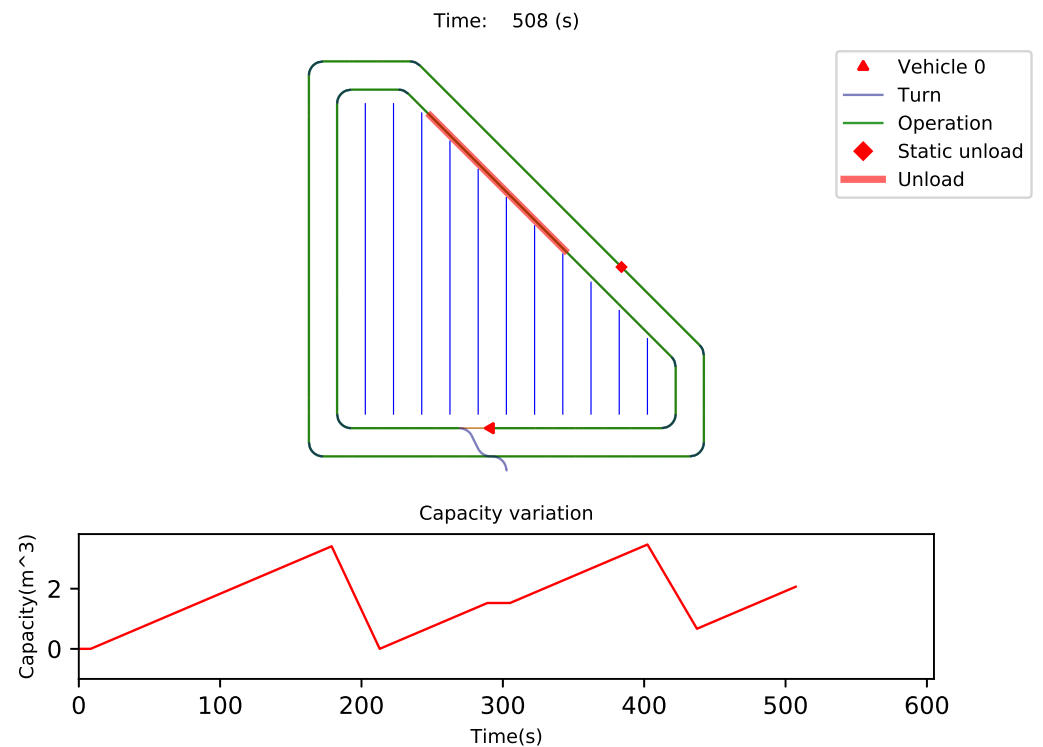


Figure 6. Headland route example with stationary and on-the-go unloading for a simplified field shape. A stationary unload is performed in the outermost headland track. An on-the-go unloading is performed in the second headland track. A clockwise driving direction is set for both headland paths. The bin level of the PU is illustrated in the diagram below the route example. Time zero is where the PU (Vehicle 0) enter the field, and 510 s is the positioning time of the PU in the route example (◄).

In order to address the shortcomings of the farm as applied track sequence patterns and to gain optimised efficiency, coverage of the primary area is generated with a meta-heuristic algorithm. It was based on the ABC algorithm for solving the capacitated vehicle routing problem (CRVP), but modified to solve the capacitated arc routing problem (CARP) [40,43]. This algorithm was developed to minimise the total route distance while generating feasible unloading actions. An example of a generated route for the primary area can be seen in Figure 7. In each step of the algorithm, modifications are made to adapt it to the CARP

and the problem formulation. Significant modifications include solution representation, generation of the initial solutions, solution cost calculation, and the use of neighbourhood operators. Existing neighbourhood operators for the CARP from Lacomme et al. [44] and Santos et al. [45] are used in combination. The output of the algorithm is a track sequence for coverage of the primary area of the field, which is mapped to a route plan, including actions such as loading. Finally, this primary area route plan is merged with the headland route plan, which in combination provides the final route plan for a complete coverage of the field. Once the complete route for the PUs is generated, the final step of the coverage path planning method is the determination of SU routes. First, all unloading actions from the PU routes are collected and used to create a list of load actions for the SUs. This list includes positions (graph arc), time, and the amount of yield (i.e., biomass in m^3) and is transferred between the PU and SU. For operations with a single PU and a single SU, the list is simply ordered by time, and a complete route can be generated for the SU, by calculating the shortest route path between load actions and inserting unloading actions for the SU when needed. For operations with multiple service units, the division of load actions between SUs is based on an optimisation of the total route distance for all SUs. The meta-heuristic algorithm described above is reused, although it uses different constraints: distance, service time, and single point unload. The distance constraint ensures that the total route distance is minimised, while the service time constraint checks that the SUs will reach all loading actions in time and not cause any delays for the PU. The single point unload constraint makes sure that each SU will travel back to a specific point (the farm depot/storage) and unload when needed. Travel to the depot and the unloading of SUs is assumed to be of a fixed duration, from each of the access points to the field. Hence, a complete route to the depot is not generated, only a route to an access point is created, where the SU will wait for the given duration. Figure 7b illustrates an SU route for the primary area, which corresponds to the PU route show in Figure 7a.

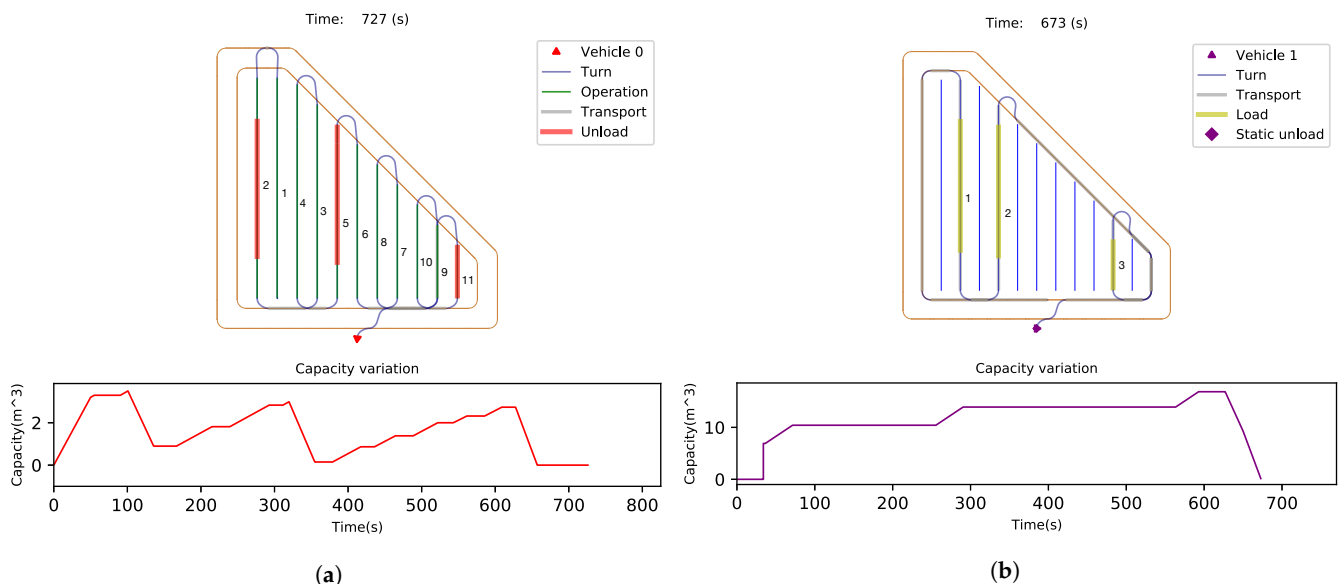


Figure 7. Coverage path planning examples for the main field area only for the PU route (a) and for a SU route (b). Three on-the-go unloadings are displayed for the simplified field shape. (a) Illustration of the track sequence of PU, where its bin level is illustrated in the diagram below the route example. Time zero is where the PU enters the field, and 727 s is the positioning time of the PU in the route example (◄), i.e., the end of harvest operation. (b) Illustration of the the track sequence of one SU, where the filling level of the transport unit is illustrated in the diagram below the route example. Depot unloading (◄) takes places where the filling level begins decreasing and ends at 673 s. Note that the time is not synchronised between the sub-figures (a,b).

The algorithm was implemented in Python technical programming language on a computer with the following specifications: Intel Core i5-3210 M CPU @ 2.50 GHZ with 4 GB RAM. The complete route plan for all PUs and SUs was stored in a proprietary format, which allowed for the generation of simulations and illustrations. However, for the analysis and comparison with the recorded data, the simulated route plans were sampled and converted to a CSV format, similar to the format and structure of the recorded data. This was accomplished to make use of identical statistical analysis methodology in order to enable a comparison of the results. The acquired data and statistical analysis are described further in the following sections.

3.3. Data Collection

3.3.1. Fields

The field recordings took place at the western part of Lolland in Denmark, between the 6 and 31 of August in 2015. The seven case study fields were sandy clay loam. In addition, the altitude of the fields derived from the Danish Agency for Data Supply and Efficiency indicated that the field topography was mainly flat. The altitude variation for a field was not more than 2 m, and the lowest and highest points of all fields were 0 and 4 m above sea level, respectively. The flatness of the seven fields did not affect machinery performance. Daily weather conditions were collected from the nearest Danish Meteorological Institute (DMI) meteorological station via Open Data Application Programming Interface (API) [46]. The 2015 regional grain harvest season was delayed in crop maturity and periodically interrupted by precipitation, providing 11 intensive days of harvest in August. Rainfall events occurred over the entire last week of July 2015 with a total of 29.4 mm of precipitation, heavy overcast, and a daily average sun radiation of 190 W/m². The monthly rainfall in August 2015 was 59 mm, which was close to normal, but the 11 days with rainfall exceeded the normal number of rainfall days in the region by 4 days. Combine harvesting was possible for 11 days in August 2015 on the farm where the recording took place. The moisture content of the harvested cereal grain varied between 13.2% and 16.0% for winter wheat and 13.6% and 15.0% for barley. The yield registrations from the combine yield sensor showed low variation within the main field area of each of the seven fields, but a slightly reduced yield level at headlands. The selected fields represent different levels of size and complexity of field shape, represented by the perimeter (m)-to-area (m²) ratio ($P/A, m^{-1}$) [47]. Table 1 shows the boundaries of the experimental fields, the crop in 2015, the area, and the P/A ratio. Field boundaries were derived from The Danish Agricultural Agency [48] in an ESRI file format for geospatial data representation.

3.3.2. Machinery and GPS Positioning System

One combine (PU) and up to two tractor and trailer (SU) combinations were involved in the experimental operations. Auto-steering systems were not used for any of the machinery generating the recorded data. The combine was a Fendt 9490X with a 10.7 m PowerFlow header type. A Fendt 930 Vario TMS tractor with 600/65-R34 front tires and 710/70-R42 rear tires, and a John Deere 6920 S AutoQuad tractor with 540/65-R28 front tires and 650/65-R38 rear tires, were used to pull identical trailers. The bogie trailer type was a Brimont BB18b with four 24-R20.5 tires and a bin size of 7.40 m (length) × 2.2 m (width) × 1.1 m (height), providing a volume of 22.8 m³. The trailer tare was 5840 kg, and the total allowed weight was 23,840 kg. The same three and highly skilled operators were involved in the harvest operations. The skills of machine operators were not considered as a factor affecting the assessment. The applied fieldwork patterns for each operation were based on the operators' own choice. Two types of GPS receivers were used for recording the positions of the vehicles involved. A Hirschmann Iridium | GNSS | 3G | GSM tri-mode combination antenna connected to an Appareo Gateway 300 with a GNSS receiver (Appareo, Italy) was used for recording and transmitting the time, position, sensor, and machine settings of the combine to the AgCommand telemetry system and server [49]. Two Aplicom A1 TRAX Data receivers with GNSS antennas (Aplicom, Finland) were used for recording

and transmitting the time and position of the service units to a server operated by Aarhus University. Both GNSS receivers provided standard GNSS as single point positioning without error corrections (<1.5 m in accuracy). Raw GNSS position data was not stored or transmitted from the telemetry systems. The recording frequency for the service units was set to 0.2 Hz to obtain sufficient resolution in-field at forward speeds up to 6 m^{-1} , and for the combine harvester, a manufacturer fixed setting of 0.1 Hz recording frequency was used. Data were downloaded from the servers as comma-separated text files. The weight of the harvested grain was measured by a weighbridge and digitally registered in a spreadsheet.

3.3.3. Decomposition of Recorded Data for Coverage Path Planning Input Parameters

The latitude and longitude data were converted to the Universal Transverse Mercator (UTM) by the KMSTrans2 tool [50] so that all data could be plotted in meters in 2D. Time was converted to epoch time for time synchronisation purposes. As the GPS recorder collected data continuously for several days, the data was divided into data-sets according to each field by a manual selection of a field-dependent interval of epoch time. Distance and forward speed were calculated between subsequent data points by using Northing (Y) and Easting (X) values. The direction of travel in degrees 0–360 was determined by first calculating the distance between subsequent data points in the Northing (Y) and Easting (X) directions individually. For obtaining a 0–360 degree scale for the direction of travel, the calculation of the degree of direction of travel was added π or $2 \cdot \pi$, depending on the sign of the distances in the X and Y directions, which affiliate the direction within quadrants of the unit circle. Stationary data points (i.e., speed $< 0.1 \text{ m}^{-1}$) were discarded, except stationary data points where combine unloading was active (combine data set included a Boolean for auger on/off). Field entrance coordinates (access points), the number of headland passes, and whether the auger was switched on when the combine was driving or stationary were all determined manually by displaying coordinates of the PU, SU, and field boundaries in QGIS [51]. All coordinates having a change in the direction of travel larger than 30° was determined as coordinates within turnings or reversing, and sorted as such. PU trajectories with more than three coordinates were determined as individual tracks, numbered and ordered in time series. The time of the headland start and end of the harvest was determined manually. The forward speed when harvesting (trajectories with yield logging > 0.1 tons/ha), the turning speed, the transport speed (yield logging = 0 tons/ha), and the average yield were determined for trajectories belonging to the headland and the main field. The average working width was determined by calculating the perpendicular distance between nearest neighbour trajectory coordinates to the left and right of a coordinate. The average working width was multiplied by the number of headland passes to provide the headland width. The following list is an overview of parameters that were passed on as input to the coverage path planning tool in relation to the PU configuration for each field:

- Field entry position (UTM E & N position)
- Field exit position (UTM E & N position)
- Headland width
- Number of headland passes
- Driving orientations at main field
- Yield, total (yield sensor)
- Yield, total (weigh bridge)
- Yield, headland
- Yield, main field
- Working width
- Forward speed, harvest, median
- Forward speed, turnings, median
- Forward speed, transport in field, upper 95%
- Total harvest time (operational only, maintenance stops not included)
- Total in-field travel distance (velocity $> 0.1 \text{ m}^{-1}$)

- No. of auger unloading when driving
- No. of auger unloading when stationary
- Unloading capacity
- Bin capacity
- Turning radius

Distance and forward speed were calculated between subsequent data points by using Northing (Y) and Easting (X) values for service units. Time series of coordinates relative to the harvest operation time interval were determined outside or inside the field polygon in order to calculate the in-field and road transport travel distance and speed, respectively. The following list is an overview of parameters that was passed on as input to the coverage path planning tool in relation to the SU configuration for each field:

- Distance from field to storage, SU1
- Distance from field to storage, SU2
- Total in-field travel distance, SU1
- Total in-field travel distance, SU2
- No. of load at weighbridge registrations
- No. of grain transports, SU1 (Fendt)
- No. of grain transports, SU2 (John Deere)
- Bin capacity, SU1 and SU2
- Unloading time duration (off-field), SU1, average
- Forward speed, transport in field, upper 99%
- Unloading time duration (off-field), SU2, average
- Forward speed, transport in field, upper 99%

3.4. Data Analysis for Comparison between Recorded and Optimised Harvest Operations

Harvest operational and non-operational distance and time were determined for PU speeds that were $>0.1 \text{ m}^{-1}$ for both the recorded data sets and similar structured data sets from the coverage path planning tool per field. The SU road transport distance between field and unloading position (e.g., grain storage) was determined for each load based on the sum of recorded distances. There was some noise to distance within a certain radius from the area of the unloading location, so all distances within a 150 m radius from the center of the unloading location were discarded from the data set. For simulated data, the number of unloadings was multiplied by the average distance between the field and unloading position derived from the recorded data. In-field distances of empty, half full, and full bins were determined directly from the simulated data sets, as the load level of the trailers was included. However, for the recorded data sets, it was necessary to combine the auger status 'on' with the nearest SU travelling at the same speed and direction as the PU. A nearest neighbour approach was used to pair PU unloadings with SUs, and the unloading capacity of 120 L/min for the PU was used to simulate and add the in-field load levels of the recorded SUs. The volume weight of spring barley (618 kg/m^3) and winter wheat (772 kg/m^3) were used to convert cubic meters of grain to kilograms of grain. The area containing traffic by SUs was determined by producing polygons of the trajectories. The trajectories were geometrically expanded to include the contact area covered by the trailer tyres.

3.5. Fuel Consumption Estimations Using ASAE Standards

The PU data sets included total fuel consumption in L/h, and a differentiation was performed based on yield intake (yield $> 0.2 \text{ tons/ha}$) in order to determine fuel consumption in L/s for harvest operation as well as for non-harvest operation per field, and only when velocity was more than 0.1 m^{-1} . The total PU fuel consumption per field was calculated by multiplying the total time in seconds by the fuel consumption in L/s for harvesting and non-harvesting, respectively. For the John Deere tractor, a fuel consumption of 242 g/kWh and 228 g/kWh was used for in-field and road operations, respectively, as different engine

revolutions occur at the two operations [52]. For the Fendt tractor, a fuel consumption of 230 g/kWh and 224 g/kWh was used for the two operations, respectively [53]. The ASAE 497.7 [54] and ASAE 496.3 [55] standards were used to calculate tractor drawbar power requirements in kW for five SU operation categories: empty trailers (in-field and road), half full trailers (in-field), and full trailers (in-field and road). Wheel load weight distribution was determined from tractor manufacturer datasheets, and the vertical weight imposed on the mechanical coupling between the tractors and the rigid trailer drawbars was estimated to be approximately 10% of the total trailer weight [56]. The average trailer weight at a full level was used for fuel consumption calculations and derived specifically from recorded as well as simulated data-sets. The average velocity per SU operation category and per field was derived from the recorded data sets. The cone index used for in-field operation was set to 900 kPa, and for asphalt, the cone index was set to 1 MPa. Wheel slip was assumed to be 5% in the field for both front and rear tractor wheels and 2% for rear tractor wheels on paved roads. The methodologies for decomposing data and determining individual PU and SU trajectories, fuel consumption, and the area with traffic was obtained in R [57]. Data management and analysis were coded using R [57].

4. Results and Discussion

It was demonstrated that path plans for both a PU and two SUs could be optimised simultaneously and simulated by the developed software executing the coverage path planning method. Prior to the actual execution of harvest operations, the method calculated the operational performance and enable to compare it with alternative machine configurations for the optimal selection and usage of the harvest fleet. The presented coverage path planning method was evaluated through a comparison between recorded CAN bus and global position data and the simulated coverage path plans. The analysis and comparison methodology described in Section 3.3 was used with data from the fields presented in Section 3.3.1. According to the recorded data, the timing of harvesting of all fields was distributed over four days. For each field, recorded data were analysed and used for parameterisation of the coverage path planning method, which was then executed, and the results were analysed and compared to the recorded data. Input parameters, such as yield map, machine capacity, maneuverability, and travel and working speeds, was derived from the recorded data in order to create a balanced comparison. Trajectory quality parameters, such as driving distances, fuel consumption, and soil compaction, was evaluated and discussed in the following. A summary of performance indicators for the comparison is presented in Tables 2 and 3. It is important to note that this case study was performed on a farm with highly skilled machine operators with many years of experience on these fields. Therefore, it is reasonable to expect that any harvest operation efficiency will become even more improved when comparing the presented coverage path planning method on data from farms with less skilled or less experienced PU and SU operators. It was observed that computational time was in fact highly exponential correlated with increase in field size, decrease in working width, increase in No. of vehicles involved in the harvest operation, and increase in unloading frequency, because the dimensional size of the solution scheme becomes larger when number of graph vertices and arcs increases. It is however anticipated that the coverage path planning method could be integrated with future auto-steering systems and terminals.

4.1. Unloading Efficiency

In order to increase field efficiency, the coverage path planning method minimised the number of on-the-go and stationary unloadings for the PU, as listed in Table 2, where the sum of all unloadings was reduced from 148 to 122 when optimisation was introduced to unload the same amount of grain as in the recorded data. The optimisation of the PU unloading strategy resulted in a reduction of stationary unloading from 15 to 9 during the entire test period. For the largest field sizes (>15 ha), the number of PU unloadings was reduced by 25%, hereof three stationary unloadings. The time savings of the reduced

unloading frequency during the four days of harvest equals an additional harvest of 1.7 ha in the same test period, when assuming the recorded average harvest capacity of 4.1 ha/h. Hence, the reduction of on-the-go and stationary unloadings did not significantly improve the field efficiency of the PU, but it reduced stress on operators for both the PU and the SUs, as on-the-go unloading requires extra attention for aligning the machines and engaging the unloading. The last column of Table 3 shows the total grain yield collected for each field. Ideally, these should be the same for the recorded data and the optimisation model; however, since the model was parameterised with an average yield for the spatial differentiation between headland and main field areas, some deviations occurred. These deviations were, however, fairly small, ranging from −6% to +5% of recorded total yield per field, where the worst deviations were seen for smaller field sizes (<15 ha).

Table 2. Comparison of the recorded (Rec.) and optimised (Opt.) number of PU unloadings, the travelled distance of SUs, the percentage of field area with traffic from SUs, the load level variation, and the number of loads per field.

Field	PU Unload		Total in-Field Distance, Service Units		Total Distance, Service Units		Area with Traffic in Percent of Total Field Area		No. of SU Transports		No. of Full Load Transports ¹		Average SU Load Level	
	Opt. []	Rec. []	Opt. [m]	Rec. [m]	Opt. [m]	Rec. [m]	Opt. [%]	Rec. [%]	Opt. []	Rec. []	Opt. []	Rec. []	Opt. [kg]	Rec. [kg]
2	12 (1)	12 (1)	9307	6224	14,424	12,315	12.9	10.5	7	9	6	0	13,072	10,651
4 ²	7 (1)	8 (1)	5537	4806	18,721	18,249	17.4	17.7	4	4	2	2	12,852	12,135
7	27 (2)	31 (3)	20,494	23,590	82,470	95,315	15.9	21.7	15	17	14	7	17,005	15,139
8	5 (0)	5 (0)	3281	3848	11,045	11,782	17.3	15.7	3	3	2	2	13,755	12,957
10	13 (1)	13 (1)	13,608	10,223	19,082	16,677	17.8	18.0	7	7	6	2	13,061	12,583
12	33 (2)	42 (5)	25,555	22,779	99,724	117,838	17.2	19.3	18	23	17	4	17,110	13,737
13 ³	16 (2)	22 (4)	16,365	18,582	110,441	123,892	16.6	22.1	9	10	7	3	17,298	15,388

¹ For spring barley, 13,500 kg was considered a full load for both registrations and simulations, where the maximum theoretical load was 14,090 kg. For winter wheat, 17,000 kg was considered a full load for both registrations and simulations, where the maximum theoretical load was 17,601 kg. ² There were two partial stationary unloading, where the unloading was initiated as on-the-go unloading. ³ Lodging at one side of the field caused harvest overlap in the opposite direction and short distance reversing providing extra harvest distance.

Table 3. Calculated SU fuel consumption and total grain yield comparison between recorded (Rec.) and simulated optimisation (Opt.) of harvest operation per field.

Field	Fuel Consumption, Service Unit A		Fuel Consumption, Service Unit B		Total Grain Yield	
	Opt. [L]	Rec. [L]	Opt. [L]	Rec. [L]	Opt. [Tons]	Rec. [Tons]
2			9.5	7.9	91.5	95.9
4			11.0	10.6	50.4	48.5
7	25.8	27.1	26.2	30.0	255.1	257.4
8			6.8	7.3	41.3	38.9
10			12.9	10.9	91.2	88.1
12	33.1	35.8	30.8	32.9	310.0	315.9
13	39.3	35.6	31.1	38.6	155.7	153.9

4.2. Transport Vehicle Efficiency

For the four smallest field sizes (i.e., <15 ha), one SU was used, and for the three largest fields (field No. 7, 12, and 13), two SUs were used because these fields were located farthest away from the grain depot. The number of service units used during the actual test period was in fact not only based on the size of the fields but also on the distance between the fields and the grain depot. The largest field sizes were incidentally also the outermost from the grain depot. The minor deviation between the total yield of recorded data and the

output from the coverage path planning method verifies that the reduction in the number of necessary SU transports as shown in Table 2 and Figure 8 was caused by a better utilisation of capacity, and not because less yield was transported in the simulation (cf. the above reflections on total yield comparison). Table 2 shows both the in-field driving distance and the total driven distance (including road transport) for both SUs. However, because of the fewer transports, the total SU travel distance was in fact reduced for fields with a distance to farm grain depot that required multiple SUs (Figure 9, Table 2). The large reduction in total distance travelled corresponding to the larger and outermost fields requiring multiple SUs was therefore primarily attributed to the lower number of SU transports between fields and the farm depot, which was further attributed by the optimised and thus better utilisation of the SU capacity (Table 2). This was evident from the analysis of average SU load level, which was improved for all fields, but most marked for the outermost fields that required two SUs, which was also the case for the number of full load transports (Table 2). The coverage path planning method was able to improve the SU full load frequency by 68% and average SU load level between 4 and 25% (field No. dependent), compared to recorded data during the test period (Table 2).

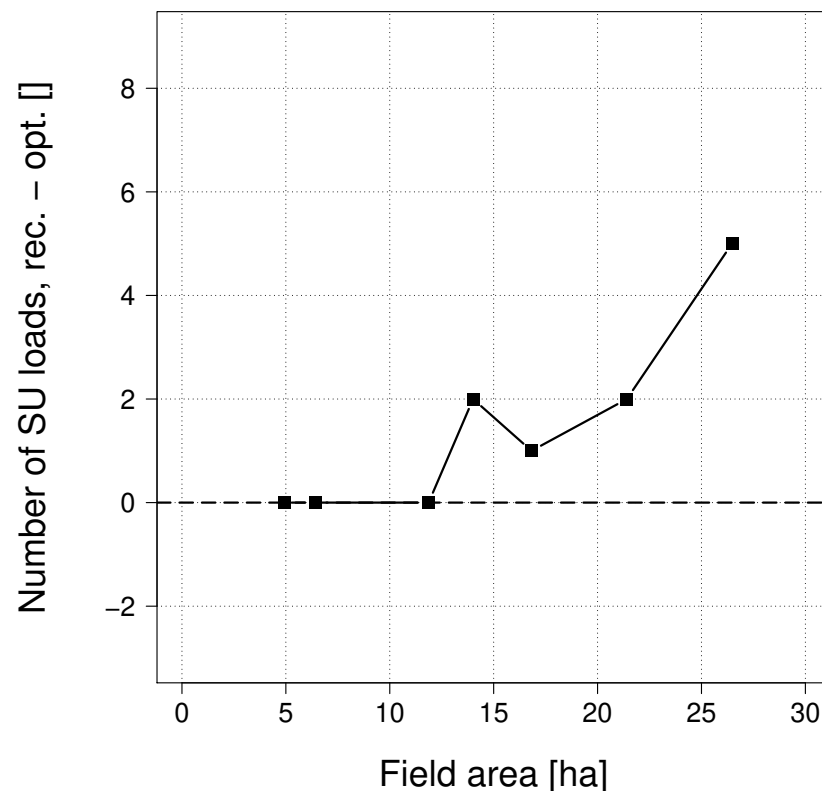


Figure 8. The difference (■) between the number of recorded SU loads and the number of SU loads optimised by the coverage path planning method in relation to field size. A difference (y-axis) is calculated per field by subtracting the number of SU loads derived from the recorded data and the number of SU loads derived from the simulated optimised route plan data. The dashed horizontal line at zero on the y-axis indicates whether the optimised route planning provided an increase or decrease in the number of SU loads compared to the recorded data, indicated by a negative or positive number of loads, respectively, in the figure.

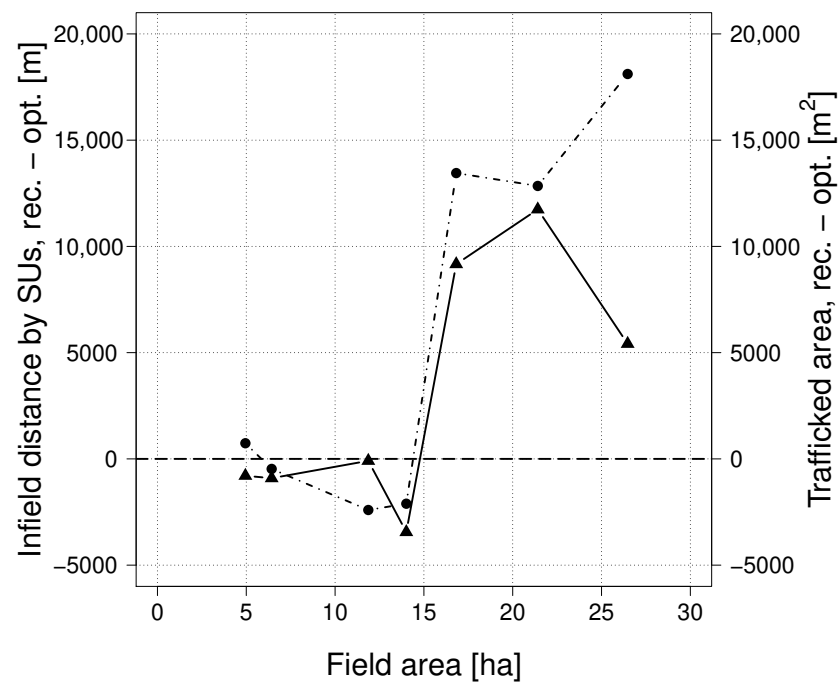


Figure 9. Differences in the total in-field travelled distance of SUs (●) and the area with traffic (▲) in relation to field size. A difference (y-axis) is calculated per field by subtracting the recorded total travelled in-field distance and the area with traffic derived from the recorded data from the total travelled in-field distance and the area with traffic derived from the simulated optimised route plan data, respectively. The dashed horizontal line at zero on the y-axis indicates whether the optimised route planning provided an increase or decrease in the total travelled in-field distance of SUs or the area with traffic compared to the results from recorded data, indicated by negative or positive in-field distances, respectively, in the figure. Note that the scale on both y axes are identical, but with different units.

4.3. CTF Model Constraint and Its Reduction in Risk of Soil Compaction

The presented coverage path planning method controlled and optimised the in-field SU routes, by minimising the total travelled distance in a CTF context. However, as shown in Figure 9, the in-field travel distance for the SUs was increased for three fields below 15 ha in size (field No. 2, 4, and 10), because of the SUs were forced to stay on the tracks defined in the field partitioning (CTF approach), whereas in the recorded data, the SUs performed U-turns in the main field area. The two different driving patterns are shown in Figure 10 for a single field, where several U-turns located in the main field area are evident for the recorded data. The implementation of CTF in the coverage path planning method, and not with the recorded data, resulted in less risk of soil compaction up to 25% (traffic limited to CTF tramlines), and at the same time reduced the in-field total travel distance up to 15% when route generation was optimised simultaneously for two SUs (Table 2). When a single SU was used, which was typically on a field smaller than 15 ha and located close to the grain depot, the implementation of controlled traffic farming (CTF) in the coverage path planning method resulted in increased area with traffic of up to 23% (traffic limited to CTF tramlines) (Figure 9) and a corresponding increase in the in-field total travel distance by 17% (Table 2). Another trade-off that was discovered, for the SUs, was the use of U-turns in the middle of the field versus the use of a CTF approach, where U-turns inside the main field were not allowed as a constraint to the coverage planning methodology. Using the CTF approach resulted in a longer in-field travel distance for the SUs, but it could also reduce in-field soil compaction, which could potentially increase yields [58,59]. The evaluation of the soil compaction risk was performed in the conducted experiment only on the simple basis of the resulting length of a trajectory and area coverage. The shorter the

trajectory was and the smaller the area with traffic, the lower the risk of soil compaction could be expected on the field level. A full expression of the relationship between trajectory and compaction is beyond the scope of this paper, but experiments have been analysed in ten Damme et al. [60], Augustin et al. [61], Pulido-Moncada et al. [62], Chyba et al. [63] and reviewed in Obour and Ugarte [64]. Figure 10 shows a comparison of in-field travel patterns for an SU in one of the fields. The frequent use of U-turns in the middle of the field in the recorded data can reduce the travel distance, but also increase the wheel covering of the main field area between tracks, compared to the CTF approach as illustrated with the example in Figure 10. The coverage path planning methodology was constrained to distribute the wheel covering and hence the load of SUs to all three headland tracks. The methodology allows for other constraint settings, for instance, to allow SU units only to travel in the track, which is used as a tramline in headland areas.

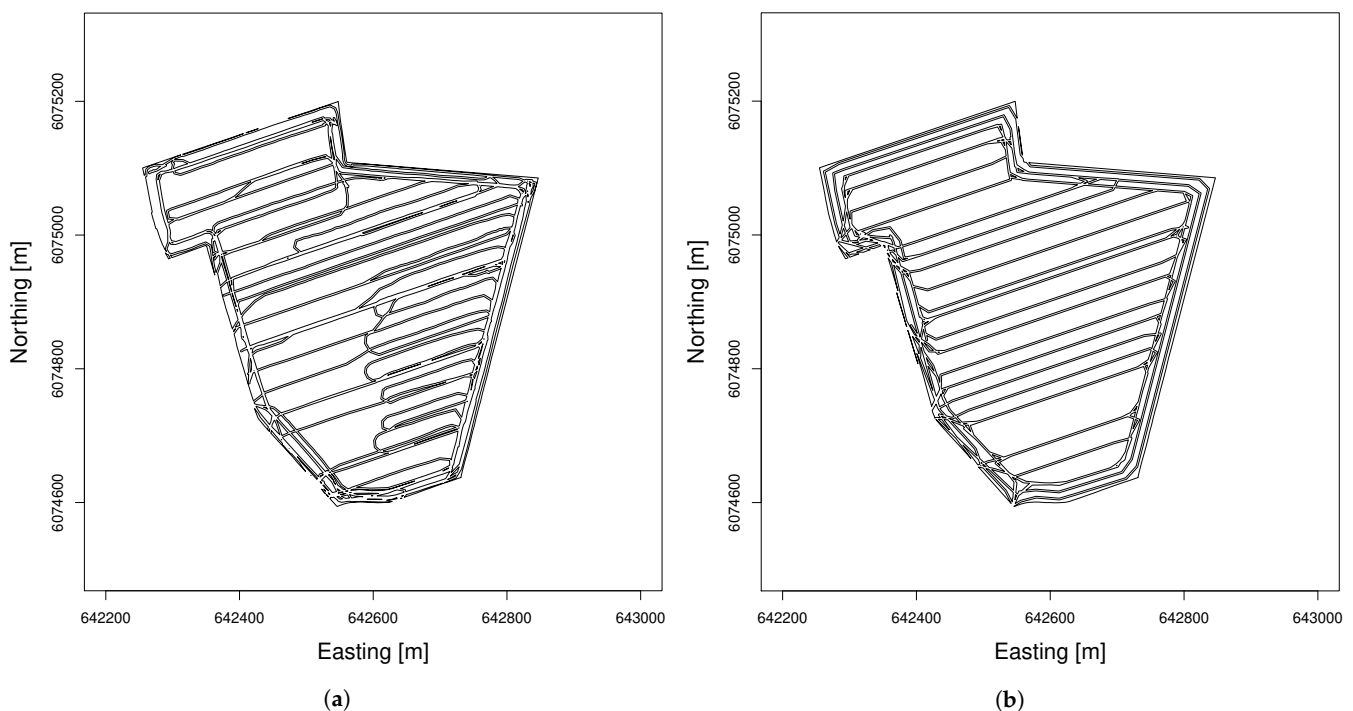


Figure 10. (a) In-field SU transport for recorded data. (b) In-field SU transport for optimised routes. Comparison of in-field area coverage with SU traffic for Field 7. Both SU A and B routes, including overlaps, are represented as coverage polygons inside the field. The simulated optimised route plan resulted in a 15.9% area coverage (b), and derived from the recorded driving of SUs the area coverage was 21.7% (a).

4.4. Fuel Efficiency

The coverage path planning method improved the SU efficiency as mentioned in Section 4.2, and the total SU travel distance was in fact reduced for fields with a distance to grain depot that required multiple SUs (Table 2). For the three fields located farthest away from the storage facility, the increase in SU full load frequency and the reduction in in-field travel distance resulted in a reduction of fuel consumption by 7% (Table 3). Findings from the fuel consumption calculation indicated that it is not sufficient to optimise the total travelled distance alone, since the fuel consumption varies significantly with the transport load and the differentiation between driving on soil and on paved road. The fuel consumption was estimated approximately 10–20% lower when driving on a paved road compared to a tilled field. In addition, the difference in fuel consumption between an empty transport unit and a fully loaded transport unit was estimated to be more than a factor of 2 for the SUs used in this study. Thus, this information could be embedded into the optimisation algorithm to reduce fuel consumption even further. It was observed that

the largest reductions in travel distance and fuel consumption were obtained at the larger fields farthest away from the grain depot, in operations where two SUs were required. This could indicate the following: (1) With an increasing distance between the field and the grain depot/storage facility, the optimisation of the given SU capacities becomes more important, as there are longer travel distances, and more fuel can thereby be saved. (2) The use of multiple SUs on larger fields is more challenging for operators, leading to more unnecessary in-field travel without a proper operator guidance system. These findings indicate that the greatest value from a coverage path planning method as the one presented can be obtained for larger and more complex operations. Subsequently, it is expected that this will also be the case when multiple PUs and SUs are used on larger fields, as this complicates the logistics chain even further.

5. Conclusions

In this study, following the logistical nature of harvest operations in an agricultural context, a coverage path planning optimisation method was developed based on the artificial bee colony (ABC) algorithm for the capacitated vehicle routing problem. In each step of the algorithm, modifications were made to adapt it to the capacitated arc routing problem, such that full coverage of the processable tracks in the graph representation of realistic field sizes was achieved and that user-defined objectives were met. It was demonstrated that the method was able to optimise the exact scheduling of the entire harvest fleet. The optimised solutions were compared with recorded data from seven fields on a Danish farm, where the harvest fleet was managed by highly experienced PU and SU operators. The method increased utilisation of SU capacities provided by a 68% increase in full load frequency and subsequently 14% reduction in total number of field to grain depot transports during the test period. The implementation of controlled traffic farming (CTF) in the coverage path planning method, but not with the recorded data, resulted in a reduced risk of soil compaction of up to 25%, and a reduction in the in-field total travel distance of up to 15% when logistics was optimised simultaneously for two transport units. For fields where logistics were optimised simultaneously for two transport units, the increase in SU full load frequency and reduction in in-field travel distance resulted in a reduction of fuel consumption by 7%. Overall, the coverage path planning method was able to provide more efficient patterns for conducting harvesting operations. The results confirmed the success of the proposed approach in obtaining more efficient logistics and transport unit capacity utilisation for harvest operations. The greatest value of the coverage path planning method will be obtained for larger and more complex operations, which could be the case when multiple PUs and SUs are used on larger fields, as this complicates the logistics chain even further. The effect of embedding the coverage path planning method software as a service, is operator stress relief, and the improved efficiency of operators, as the system in front of the operator calculates and displays all required actions from the operator, and each operator are then frequently and exactly informed about when and where the next unloading must take place. This approach is also applicable in operation planning for autonomous vehicles. For future studies, the coverage path planning method could be extended by assuming other constraints or conditions in agricultural fleet management. For example, all input data of the proposed model was deterministic. The model could be developed to support stochastic conditions, such as spatial crop yield rates.

Author Contributions: Methodology, R.S.N. and M.N.; software, R.S.N.; validation, R.S.N. and M.N.; analysis, M.N.; data curation, R.S.N. and M.N.; writing—original draft preparation, R.S.N., M.N. and C.A.G.S.; writing—review and editing, M.N.; visualisation, R.S.N. and M.N.; supervision, C.A.G.S. All authors have read and agreed to the published version of the manuscript.

Funding: This research was funded by the Danish Innovation Foundation and AGCO A/S (the ‘Off-line and on-line logistics planning of harvesting processes’ project, grant number 7038-00249B).

Institutional Review Board Statement: Not applicable.

Informed Consent Statement: Not applicable.

Data Availability Statement: The recorded and simulation data are available on request from the corresponding author.

Acknowledgments: This article was written with support from the the Danish Innovation Foundation and AGCO A/S (the ‘Off-line and on-line logistics planning of harvesting processes’ project, grant number 7038-00249B). The authors thank the farm employees, estate owner, and local machinery marketing for the disposal of fields, machinery, and absolute yield registrations (i.e., weighing bridge data).

Conflicts of Interest: The authors declare that there are no conflict of interest. A co-funding agreement for joint research and development between Aarhus University and AGCO A/S was signed.

References

1. Dos Reis, A.V.; Medeiros, F.A.; Ferreira, M.F.; Machado, R.L.T.; Romano, L.N.; Marini, V.K.; Francetto, T.R.; Tavares Machado, A.L. Technological trends in digital agriculture and their impact on agricultural machinery development practices. *Rev. Cienc. Agron.* **2020**, *51*, 1–12. [\[CrossRef\]](#)
2. Blackmore, S.; Griepentrog, H.W. *Autonomous Vehicles and Robotics*; CIGR Handbook of Agricultural Engineering Volume VI Information Technology; Chapter 4 Mechatronics and Applications; Munaxk, A., Ed.; ASABE: St. Joseph, MI, USA, 2006. [\[CrossRef\]](#)
3. Sørensen, C.A.G.; Bochtis, D.D. Conceptual model of fleet management in agriculture. *Biosyst. Eng.* **2010**, *105*, 41–50. [\[CrossRef\]](#)
4. Bochtis, D.D.; Sørensen, C.A.G.; Busato, P. Advances in agricultural machinery management: A review. *Biosyst. Eng.* **2014**, *126*, 69–81. [\[CrossRef\]](#)
5. Saiz-Rubio, V.; Rovira-Mas, F. From Smart Farming towards Agriculture 5.0: A Review on Crop Data Management. *Agriculture* **2020**, *10*, 207. [\[CrossRef\]](#)
6. Ansoorge, D.; Godwin, R.J. The effect of tyres and a rubber track at high axle loads on soil compaction, Part 1: Single axle-studies. *Biosyst. Eng.* **2007**, *98*, 115–126. [\[CrossRef\]](#)
7. Ansoorge, D.; Godwin, R.J. The effect of tyres and a rubber track at high axle loads on soil compaction—Part 2: Multi-axle machine studies. *Biosyst. Eng.* **2008**, *99*, 338–347. [\[CrossRef\]](#)
8. Vahdanjoo, M.; Zhou, K.; Sørensen, C.A.G. Route Planning for Agricultural Machines with Multiple Depots: Manure Application Case Study. *Agriculture* **2020**, *10*, 1608. [\[CrossRef\]](#)
9. Jensen, M.F.; Bochtis, D.D.; Sørensen, C.G. Coverage planning for capacitated field operations, part II: Optimisation. *Biosyst. Eng.* **2015**, *139*, 149–164. [\[CrossRef\]](#)
10. Edwards, G.T.C.; Hinge, J.; Skou-Nielsen, N.; Villa-Henriksen, A.; Sørensen, C.A.G.; Green, O. Route planning evaluation of a prototype optimised infield route planner for neutral material flow agricultural operations. *Biosyst. Eng.* **2017**, *153*, 149–157. [\[CrossRef\]](#)
11. Rodias, E.; Berruto, R.; Busato, P.; Bochtis, D.D.; Sørensen, C.G.; Zhou, K. Energy Savings from Optimised In-Field Route Planning for Agricultural Machinery. *Sustainability* **2017**, *9*, 1956. [\[CrossRef\]](#)
12. Utamima, A.; Reiners, T.; Ansariipoor, A.H. Optimisation of agricultural routing planning in field logistics with Evolutionary Hybrid Neighbourhood Search. *Biosyst. Eng.* **2019**, *184*, 166–180. [\[CrossRef\]](#)
13. Jensen, M.A.F.; Bochtis, D.D.; Sørensen, C.G.; Blas, M.R.; Lykkegaard, K.L. In-field and inter-field path planning for agricultural transport units. *Comput. Electron. Agric.* **2012**, *63*, 1054–1061. [\[CrossRef\]](#)
14. Guevara, L.; Rocha, R.P.; Cheein, F.A. Improving the manual harvesting operation efficiency by coordinating a fleet of N-trailer vehicles. *Comput. Electron. Agric.* **2021**, *185*, 106103. [\[CrossRef\]](#)
15. Conesa-Munoz, J.; Pajares, G.; Ribeiro, A. Mix-opt: A new route operator for optimal coverage path planning for a fleet in an agricultural environment. *Expert Syst. Appl.* **2016**, *54*, 364–378. [\[CrossRef\]](#)
16. Jin, J.; Tang, L. Optimal coverage path planning for arable farming on 2D surfaces. *Trans. ASABE* **2010**, *53*, 283–295. [\[CrossRef\]](#)
17. Oksanen, T.; Visala, A. Coverage Path Planning Algorithms for Agricultural Field Machines. *J. Field Robot.* **2009**, *26*, 651–668. [\[CrossRef\]](#)
18. Zhou, K.; Jensen, A.L.; Sørensen, C.G.; Busato, P.; Bochtis, D.D. Agricultural operations planning in fields with multiple obstacle areas. *Comput. Electron. Agric.* **2014**, *109*, 12–22. [\[CrossRef\]](#)
19. Hameed, I.A. Intelligent Coverage Path Planning for Agricultural Robots and Autonomous Machines on Three-Dimensional Terrain. *J. Intell. Robot. Syst.* **2014**, *74*, 965–983. [\[CrossRef\]](#)
20. Jin, J.; Tang, L. Coverage Path Planning on Three-Dimensional Terrain for Arable Farming. *J. Field Robot.* **2011**, *28*, 424–440. [\[CrossRef\]](#)
21. Reznik, T.; Herman, L.; Klocova, M.; Leitner, F.; Pavelka, T.; Leitgeb, S.; Trojanova, K.; Stampach, R.; Moshou, D.; Mouazen, A.M.; et al. Towards the Development and Verification of a 3D-Based Advanced Optimized Farm Machinery Trajectory Algorithm. *Sensors* **2021**, *21*, 2980. [\[CrossRef\]](#)

22. Bochtis, D.D.; Sørensen, C.G.; Green, O. A DSS for planning of soil-sensitive field operations. *Decis. Support Syst.* **2012**, *53*, 66–75. [\[CrossRef\]](#)
23. Villa-Henriksen, A.; Skou-Nielsen, N.; Munkholm, L.J.; Sørensen, C.A.G.; Green, O.; Edwards, G.T.C. Infield optimized route planning in harvesting operations for risk of soil compaction reduction. *Soil Use Manag.* **2021**, *37*, 810–821. [\[CrossRef\]](#)
24. Spekken, M.; de Bruin, S. Optimized routing on agricultural fields by minimizing maneuvering and servicing time. *Precis. Agric.* **2013**, *14*, 224–244. [\[CrossRef\]](#)
25. Grisso, R.; Jasa, P.; Rolofson, D. Analysis of traffic patterns and yield monitor data for field efficiency determination. *Appl. Eng. Agric.* **2002**, *18*, 171–178. [\[CrossRef\]](#)
26. Isaac, N.; Quick, G.; Birrell, S.; Edwards, W.; Coers, B. Combine harvester econometric model with forward speed optimization. *Appl. Eng. Agric.* **2006**, *22*, 25–31. [\[CrossRef\]](#)
27. Bochtis, D.D.; Sørensen, C.G.; Green, O.; Moshou, D.; Olesen, J. Effect of controlled traffic on field efficiency. *Biosyst. Eng.* **2010**, *106*, 14–25. [\[CrossRef\]](#)
28. Taylor, R.; Schrock, M.; Staggenborg, S. Extracting Machinery Management Information from GPS Data. In *ASAE Meeting Paper No.: 02-1008, Proceedings of the ASAE Annual International Meeting, Chicago, IL, USA, 28–31 July 2002*; ASAE: St. Joseph, MI, USA, 2002. [\[CrossRef\]](#)
29. Jensen, M.F.; Nørremark, M.; Busato, P.; Sørensen, C.G.; Bochtis, D.D. Coverage planning for capacitated field operations, Part I: Task decomposition. *Biosyst. Eng.* **2015**, *139*, 136–148. [\[CrossRef\]](#)
30. de Bruin, S.; Lerink, P.; La Riviere, I.J.; Vanmeulebrouk, B. Systematic planning and cultivation of agricultural fields using a geo-spatial arable field optimization service: Opportunities and obstacles. *Biosyst. Eng.* **2014**, *120*, 15–24. [\[CrossRef\]](#)
31. Seyyedhasani, H.; Dvorak, J.S. Reducing field work time using fleet routing optimization. *Biosyst. Eng.* **2018**, *169*, 1–10. [\[CrossRef\]](#)
32. Bakhtiari, A.; Navid, H.; Mehri, J.; Berruto, R.; Bochtis, D.D. Operations planning for agricultural harvesters using ant colony optimization. *Span. J. Agric. Res.* **2013**, *11*, 652–660. [\[CrossRef\]](#)
33. Bochtis, D.D.; Sørensen, C.G.; Jorgensen, R.N.; Green, O. Modelling of material handling operations using controlled traffic. *Biosyst. Eng.* **2009**, *103*, 397–408. [\[CrossRef\]](#)
34. Evans, J.T.; Pitla, S.K.; Luck, J.D.; Kocher, M. Row crop grain harvester path optimization in headland patterns. *Comput. Electron. Agric.* **2020**, *171*, 105295. [\[CrossRef\]](#)
35. Ali, O.; Verlinden, B.; Van Oudheusden, D. Infield logistics planning for crop-harvesting operations. *Eng. Optim.* **2009**, *41*, 183–197. [\[CrossRef\]](#)
36. Bochtis, D.D.; Sørensen, C.G.; Busato, P.; Berruto, R. Benefits from optimal route planning based on B-patterns. *Biosyst. Eng.* **2013**, *115*, 389–395. [\[CrossRef\]](#)
37. Bochtis, D.D.; Sørensen, C.G. The vehicle routing problem in field logistics: Part I. *Biosyst. Eng.* **2009**, *104*, 447–457. [\[CrossRef\]](#)
38. Bochtis, D.D.; Sørensen, C.G.; Vougioukas, S.G. Path planning for in-field navigation-aiding of service units. *Comput. Electron. Agric.* **2010**, *74*, 80–90. [\[CrossRef\]](#)
39. Nilsson, R.S.; Zhou, K. Decision Support Tool for Operational Planning of Field Operations. *Agriculture* **2020**, *10*, 229. [\[CrossRef\]](#)
40. Nilsson, R.S.; Zhou, K. Method and bench-marking framework for coverage path planning in arable farming. *Biosyst. Eng.* **2020**, *198*, 248–265. [\[CrossRef\]](#)
41. Dubins, L.E. On curves of minimal length with a constraint on average curvature, and with prescribed initial and terminal positions and tangents. *Am. J. Math.* **1957**, *79*, 497–516. [\[CrossRef\]](#)
42. Dijkstra, E. A note on two problems in connexion with graphs. *Numer. Math.* **1959**, *1*, 269–271. [\[CrossRef\]](#)
43. Szeto, W.Y.; Wu, Y.; Ho, S.C. An artificial bee colony algorithm for the capacitated vehicle routing problem. *Eur. J. Oper. Res.* **2011**, *215*, 126–135. [\[CrossRef\]](#)
44. Lacomme, P.; Prins, C.; Ramdane-Sherif, W. Competitive memetic algorithms for arc routing problems. *Ann. Oper. Res.* **2004**, *131*, 159–185. [\[CrossRef\]](#)
45. Santos, L.; Coutinho-Rodrigues, J.; Current, J.R. An improved ant colony optimization based algorithm for the capacitated arc routing problem. *Transport Res. B Meth.* **2010**, *44*, 246–266. [\[CrossRef\]](#)
46. The Danish Meteorological Institute. The Danish Meteorological Institute's (DMI) Open Data API Provides Free and Open Access to Weather Stations in Denmark and Greenland. Available online: <https://confluence.govcloud.dk/display/FDAPI/Danish+Meteorological+Institute+-+Open+Data> (accessed on 28 April 2022).
47. Luck, J.D.; Zandonadi, R.S.; Shearer, S.A. A case study to evaluate field shape factors for estimating overlap errors with manual and automatic section control. *Trans. ASABE* **2011**, *54*, 1237–1243. [\[CrossRef\]](#)
48. The Danish Agricultural Agency. Field Polygons for the Growing Season 2015. Available online: <https://landbrugsgeodata.fvm.dk/> (last accessed on 25 April 2022).
49. AGCO Corporation. AgCommand Telemetry System. Available online: <http://myagcommand.com/AgcommandPortal/agcommand/fleet.html> (accessed on 25 September 2017).
50. KMStrans2—A Danish Coordinate Conversion Tool. Available online: <https://sdfe.dk/saadan-arbejder-vi-med-data/geodaesi-og-referencenet/koordinattransformation/> (accessed on 30 June 2017).
51. QGIS Development Team. *QGIS Geographic Information System*; Open Source Geospatial Foundation Project: Chicago, IL, USA, 2016.

52. DLG-Prüfstelle für Landmaschinen. John Deere 6920 S AutoQuad. In *OECD-Test Nr. 07/2002*; Deutsche Landwirtschafts-Gesellschaft–German Agricultural Society (DLG): Frankfurt, Germany, 2002; Volume 2. Available online: https://pruefberichte.dlg.org/filestorage/JDEERE_6620_AutoQuad_Nr7-2002.pdf (accessed on 25 April 2022).
53. DLG-Testzentrum Technik und Betriebsmittel. Fendt 930 Vario TMS. In *DLG-profi Test Heft Nr. 04/2004*; Deutsche Landwirtschafts-Gesellschaft–German Agricultural Society (DLG): Frankfurt, Germany, 2004; Volume 4. Available online: https://pruefberichte.dlg.org/filestorage/pbdocs/traktoren/Fendt930VarioTMS_2004.pdf (accessed on 25 April 2022).
54. *Standard ASAE D497.7*; Agricultural Machinery Management Data. American Society of Agricultural and Biological Engineers: St. Joseph, MI, USA, 2015.
55. *Standard ASAE EP496.3*; Agricultural Machinery Management. American Society of Agricultural and Biological Engineers: St. Joseph, MI, USA, 2015.
56. United Nations. *Regulation No. 147-00. Mechanical Coupling Components of Combinations of Agricultural Vehicles*; ECE/TRANS/WP.29/2018/69; United Nations: Rome, Italy, 2019.
57. R Core Team. *R: A Language and Environment for Statistical Computing*; R Core Team: Vienna, Austria, 2013.
58. Antille, D.L.; Peets, S.; Galambošová, J.; Botta, G.F.; Rataj, V.; Macak, M.; Tullberg, J.N.; Chamen, W.C.T.; White, D.R.; Misiewicz, P.A.; et al. Review: Soil compaction and controlled traffic farming in arable and grass cropping systems. *Agron. Res.* **2019**, *17*, 653–682. [[CrossRef](#)]
59. Rataj, V.; Kumhalova, J.; Macak, M.; Barat, M.; Galambosova, J.; Chyba, J.; Kumhala, F. Long-Term Monitoring of Different Field Traffic Management Practices in Cereals Production with Support of Satellite Images and Yield Data in Context of Climate Change. *Agronomy* **2022**, *12*, 128. [[CrossRef](#)]
60. Ten Damme, L.; Schjønning, P.; Munkholm, L.J.; Green, O.; Nielsen, S.K.; Lamande, M. Soil structure response to field traffic: Effects of traction and repeated wheeling. *Soil Tillage Res.* **2021**, *213*, 105128. [[CrossRef](#)]
61. Augustin, K.; Kuhwald, M.; Brunotte, J.; Duttmann, R. Wheel Load and Wheel Pass Frequency as Indicators for Soil Compaction Risk: A Four-Year Analysis of Traffic Intensity at Field Scale. *Geosciences* **2020**, *10*, 292. [[CrossRef](#)]
62. Pulido-Moncada, M.; Munkholm, L.J.; Schjønning, P. Wheel load, repeated wheeling, and traction effects on subsoil compaction in northern Europe. *Soil Tillage Res.* **2019**, *186*, 300–309. [[CrossRef](#)]
63. Chyba, J.; Kroulik, M.; Křištof, K.; Misiewicz, P. The influence of agricultural traffic on soil infiltration rates. *Agron. Res.* **2017**, *15*, 664–673. Available online: <http://agronomy.emu.ee/index.php/category/volume-15-2017/number-3-volume-15-2017/?aid=5390&sa=0#abstract-5453> (accessed on 11 April 2022).
64. Obour, P.B.; Ugarte, C.M. A meta-analysis of the impact of traffic-induced compaction on soil physical properties and grain yield. *Soil Tillage Res.* **2021**, *211*. [[CrossRef](#)]